



*Anal. Bioanal. Chem. Res., Vol. 9, No. 1, 123-132, January 2022.*

## One-step Green Synthesis of Highly Luminescent Carbon Dots from Beef and Application as Selective and Sensitive Nanosensor for Ketotifen Fumarate Detection in Human Serum and Urine Samples

Mahshid Olfati Sumar<sup>a</sup>, Naser Samadi<sup>b,\*</sup>, Mohsen Irandoust<sup>a</sup> and Saeedeh Narimani<sup>b</sup>

<sup>a</sup>Department of Analytical Chemistry, Faculty of Chemistry, Razi University, Kermanshah, Iran

<sup>b</sup>Department of Chemistry, Faculty of Science, Urmia University, Urmia, Iran

(Received 4 March 2021 Accepted 21 September 2021)

Green luminescent water-soluble carbon dots (CDs); were synthesized by the simple one-step hydrothermal method of: beef, shrimp, beef liver and, oyster, without using a surface passivating and oxidizing agents or inorganic salts. The application of high fluorescent beef CDs; without surface modification was described as a green, simple, and inexpensive method for sensitive and selective determination of ketotifen fumarate (KTF) based on fluorescent quenching. The beef CDs exhibit exceptional advantages, including: significant fluorescent quantum yield (13.75), and, admissible chemical stability. The quantum yields of CDs from beef, oyster, beef liver, and shrimp were calculated as: 13.75, 17.29, 20.59, and 17.45, respectively. Among the prepared CDs, only the fluorescence of CDs prepared from beef was significantly reduced by KTF, indicating the high selectivity of beef CDs toward KTF. The linear range of determination of KTF by this nanosensor was  $7.00 \times 10^{-7}$ - $5.00 \times 10^{-6}$  M with a detection limit of 0.30  $\mu$ M. The proposed method was then applied to the highly sensitive and selective determination of KTF in human serum and urine samples with acceptable results.

**Keywords:** Carbon Dots, Ketotifen Fumarate, Beef, Fluorescence Quenching

### INTRODUCTION

Fluorescent carbon dots (CDs); a new member of the carbon-based nanomaterial family with sizes below 10 nm, were discovered in 2004 through the purification of single-walled carbon nanotubes by preparative electrophoresis. They have captured increasing attention because of their exclusive photo-luminescence properties, excellent surface effect, chemical and, photostability, high quantum yield, insignificant cytotoxicity and, acceptable biocompatibility [1-4]. As a result, CDs; were widely applied in fluorescent sensors, cell imaging, determination of metal cations and drugs, detection of organophosphate pesticides, *etc.* [5-7]. Ketotifen is the second-generation non-competitive H<sub>1</sub> blocker antihistamine and is most often

accessible as a salt of fumaric acid (ketotifen fumarate) [8-12]. It is generally received as an anti-asthmatic/anti anaphylactic drug and assuages allergic disorders via an alliance of several actions, such as, a non-competitive antagonist of histamine H<sub>1</sub> receptors and, is a mast cell stabilizer, inhibiting the release of inflammatory mediators from mast cells [13-15].

Side effects of ketotifen fumarate (KTF) include drowsiness, blurred vision, weight gain, dry mouth, fast pounding or irregular heartbeat or pulse, chills, irritability and, increased nosebleeds [16]. The therapeutic importance of the drug has been promoted to expand different techniques for its assay in human fluids, such as high-performance liquid chromatography [17-24], spectrofluorimetry [25], UV spectrometry [26,27], coulometric titration [28], chemiluminescence (CL) detection [29], and potentiometric titration [30]. Because

Corresponding author. E-mail: Samadi76@yahoo.com

other methods of measuring ketotifen fumarate, such as chromatography, are complex and require an operator, a nanosensor was developed here based on CDs; that have features such as low toxicity, ease of preparation, high fluorescence, optical properties depending on the surface chemistry, and accessible to functionalization.

In this work, a simple, economical and green, method was made for the synthesis of CDs; from beef, beef liver, shrimp and, oyster. This is a complex material that consists of several organics and biomolecules such as fat, proteins, vitamin B, vitamin C, vitamin E, carbohydrates, cholesterol, and minerals, which can be effective for doping of multiple heteroatoms in CDs; without any surface passivation. As far as the authors know, the determination of ketotifen fumarate (KTF) using CDs; as a sensitive nanoprobe has not been reported in the literature. According to this finding, beef CDs; as a fluorescent quenching method were constructed for selective determination of ketotifen fumarate in human serum and urine samples.

## MATERIALS AND METHODS

### Reagents

Raw materials including: beef, shrimp, beef liver and oyster, were obtained from the local market. Vancomycin, isoniazid, meropenem, acetaminophen, cloxacillin, sulfonamide, ibuprofen and, ceftriaxone were purchased from Sigma-Aldrich (Germany). All amino acids and metal salts such as  $\text{Na}_2\text{SO}_4$ ,  $\text{Mg}(\text{NO}_3)_2 \cdot 6\text{H}_2\text{O}$ ,  $\text{Zn}(\text{NO}_3)_2 \cdot 4\text{H}_2\text{O}$ ,  $\text{Ca}(\text{NO}_3)_2 \cdot 4\text{H}_2\text{O}$  and,  $\text{MnCl}_2 \cdot 4\text{H}_2\text{O}$  were obtained from Merck (Germany). Double-distilled deionized water to prepare all the solution in this study was used. (Obtained from Ghazi serum co., Tabriz, Iran). Triphenylphosphine ( $\text{pph}_3$ ) was purchased from Merck (Darmstadt, Germany). Ketotifen fumarate (KTF) standard solution with a concentration of 0.10 mM was prepared daily using a suitable amount of KTF drug (Behsa, Iran). The required solutions of the KTF at other concentrations were obtained by diluting the stock solution.  $\text{KH}_2\text{PO}_4$  and  $\text{K}_2\text{HPO}_4$  were used to preparing buffer solutions. All other reagents were of analytical grade from Merck (Darmstadt, Germany).

### Apparatus

The JASCO fluorescence spectrometer model FP-PC-

6500 was used to characterize and investigate the fluorescence of CDs. The spectral band path was set at 10 nm. The size and shape of CDs nanoparticles were determined by high-resolution transmission electron microscopy (HR-TEM CM30) at 300 kv. UV-Vis absorption spectra were recorded using a Bichrom II spectrometer. Fourier transform infrared (FT-IR) spectra of the CDs were measured using a NEXUS 670FTIR spectrometer with the KBr pellet technique. The ALPHA-CHRIST dry freezing was used to freeze-drying CDs (Germany). Zeta potential and dynamic light scattering (DLS) were measured by a zeta sizer nano ZS (red badye) ZEN 3600(DLS) (Malvern, U, K).

### Synthesis of CDs

These sections of the report present a method of preparing four batches of CDs; from natural materials, including: beef, beef liver, shrimp and, oyster. CDs; were constructed using the hydrothermal method. For this purpose, during the four steps, four CDs; were prepared separately from: beef, beef liver, shrimp and, oyster according to the following method. 20 g of the above-mentioned materials were thoroughly crushed by a mixer and transferred to a Teflon-lined stainless steel autoclave with 150 ml of water. The autoclave was heated by an oven at 200 °C for 10 h. After cooling naturally to room temperature, the suspension was centrifuged at 10000 rpm for 10 min. after settling additives, a brown solution was collected (for obtained). In order to obtain pure CDs, the solution was filtered through a 0.22  $\mu\text{m}$  cellulose acetate filter and was kept at 4 °C for further use. In order to more maintenance and stability of solutions and to record the FT-IR spectra, the solutions of CDs were freeze-dried.

### Quantum Yield Measurement

The Quinine sulfate was selected as the standard to determine the quantum yield (QY); of the synthesized CDs. QY; of four CDs; was compared to quinine sulfate as a reference with a QY; of 0.54 in solution of sulfuric acid 0.50 M using the following equation at 330 nm:

$$\phi_x = \phi_r (I_x / I_r) (A_r / A_x) (\eta_x^2 / \eta_r^2) \quad (1)$$

Where  $\phi_r$  and  $\phi_x$  are the quantum yield of quinine sulfate

and beef CDs, respectively. I represent the integrated emission spectra: A is absorbance,  $\eta$  is the refractive index of the solvent and, r and x represent to standard and sample, respectively (Fig. 2a). The absorption was kept below 0.10 at the excitation wavelength (330 nm), to minimize re-absorption effects [31].

### General Fluorescence Measurements

The measure fluorescence, 1 ml of CDs solution and, 1 ml of  $7.00 \times 10^{-3}$  M phosphate buffer solution (pH = 8) were added to different concentrations of ketotifen fumarate and the final volume of the mixture was adjusted to 5.0 ml with deionized water. All measurements were performed immediately at room temperature. The fluorescence intensity was recorded at 416 nm with an excitation wavelength of 330 nm.

### Preparation of Real Samples

Human plasma samples were obtained from the hospital (Urmia). A 5 ml aliquot of plasma was placed into the centrifuged tube and, 40  $\mu$ l of 0.20 M HCl and 20  $\mu$ l of 0.40 M  $\text{pph}_3$  were added into it and, vigorously mixed. After incubating for 20 min, 0.50 ml of acetonitrile was added into the obtained hydrolyzed plasma to precipitate proteins. The solution was centrifuged for 15 min and the supernatant solution was transferred into a 10 ml volumetric flask and diluted to the mark with deionized water.

Urine samples were collected and centrifuged (10000 rpm, 15 min) to precipitate impurities. Then, the supernatant was diluted 100-fold with deionized water. All real samples were collected from healthy volunteers.

## RESULTS AND DISCUSSION

### Characterization of CDs

The morphology and size of the CDs were confirmed by TEM and DLS measurements. Figure 1a shows a TEM image of the as-prepared CDs made from beef, which are mostly spherical and separable. Size distribution of the beef CDs (Fig. S1a), indicates that the majority of the nanoparticles are between 1-4 nm in hydrodynamic diameter. The as-prepared CDs from the beef have good stability due to their zeta potential higher than +30 mV

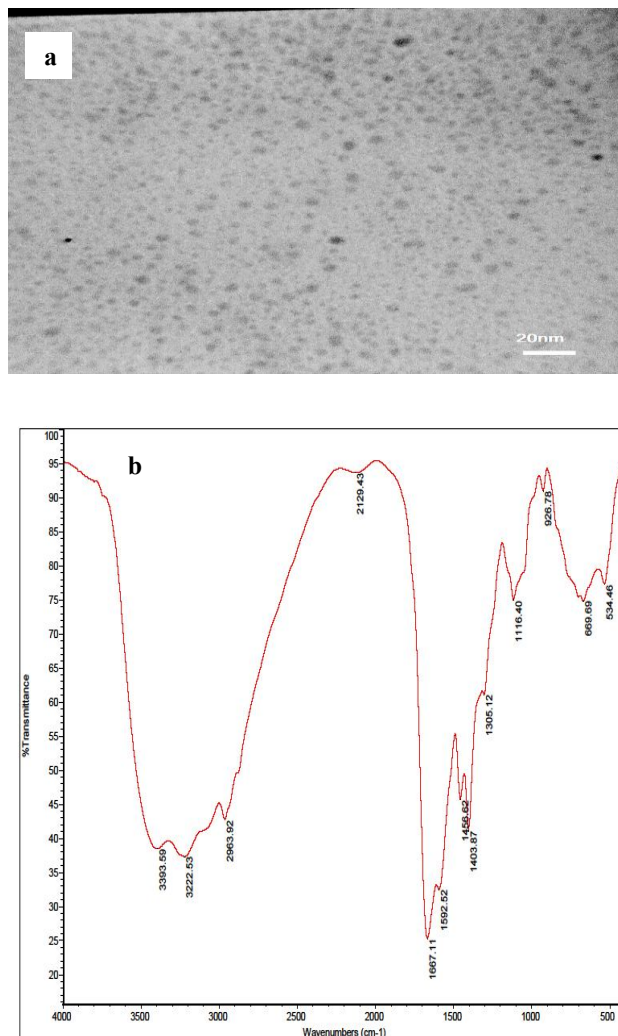


Fig. 1. (a) TEM image and (b) FT-IR of beef CDs.

(about +100 mV), the probability of aggregation, and a meager particle size increase (Fig. S1b) [32,33]. The functional groups present on the surface of the beef CDs were investigated using FT-IR spectroscopy. Also, figure (S2) shows FT-IR spectra of the as-prepared CDs made from the beef liver, shrimp and, oyster.

A broad, intense band can be seen at  $3393\text{ cm}^{-1}$ , corresponding to O-H stretching vibrations. An intense band corresponding to N-H stretching vibration of amino groups can be seen at  $1592\text{ cm}^{-1}$ . A band attributed to the C-OH stretching vibration can be observed at  $1305\text{ cm}^{-1}$ . The band at about  $2963\text{ cm}^{-1}$  is related to the stretching vibration of

C-H. The band at  $1667\text{ cm}^{-1}$  belongs to the C=O stretching vibration. The band in  $1400\text{-}1600\text{ cm}^{-1}$  corresponds to the stretching vibrations for C=C in aromatic hydrocarbons (Fig. 1b) [34-36]. The presence of these functional groups indicates the excellent solubility of CDs in water, and these characteristic bands verify the successful formation of CDs. Figure (S3) depicts the TEM images of CDs made from them: beef liver, shrimp, and, oyster, respectively. As can be seen in the figures, the produced CDs are mostly spherical and, separable.

### Optical Properties

The investigated optical properties of the prepared CDs were UV-Vis absorption, excitation fluorescence emission and QY. UV-Vis spectra were recorded by a spectrophotometer in the range of 200-7500. As can be seen in Fig. 2b, the absorption peak of CDs from the beef seen at 265 nm is assigned to the  $\pi\text{-}\pi^*$  transition of the aromatic  $\text{sp}^2$  domains [37]. One evidence for the formation of the CDs is the presence of the photoluminescence spectra. The as-prepared CDs exhibited considerable blue photoluminescence when illuminated under a UV lamp, indicating the formation of luminescence carbon nanoparticles [38]. A narrow fluorescence peak is seen at about 416 nm (Fig. 2b) when the CDs produced by the beef are excited by a 330 nm wavelength. A quantum yield of 13.75% was calculated for beef CDs using quinine sulfate as the reference. This quantum yield value is notably higher than those of many reported luminescent CDs made from natural material [39-43] (Fig. 2a). The changes in the fluorescence emission intensity of CDs due to the excitation wavelength changes were investigated to determine the dependence of the emission spectrum on the excitation wavelength. To determine the maximum emission wavelength, the maximum value of the fluorescence emission wavelength was determined by changing the excitation wavelength in the range of 300-380 nm, determined (Fig. S4). The intensity of fluorescence emission depends on the number of excited particles at specific wavelengths. Another factor that can be effective in this intrinsic behavior is the presence of different functional groups at the surface of CDs. The combination of the molecular orbitals of these functional groups with the carbon core electron orbitals can create new energy levels,

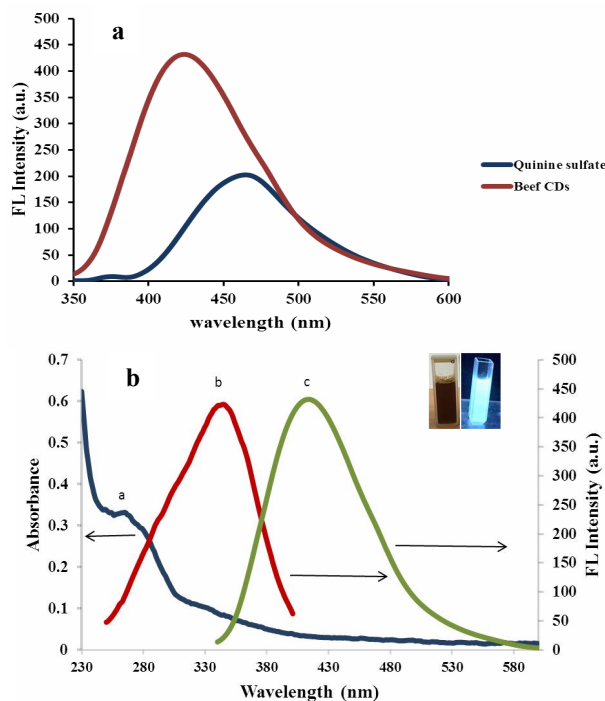


**Fig. 2.** (a) Comparison of fluorescence emission spectra of the beef CDs and quinine sulfate. (b) UV-Vis absorption, excitation ( $\lambda_{\text{em}} = 416\text{ nm}$ ) and fluorescence ( $\lambda_{\text{em}} = 330\text{ nm}$ ) emission spectra of beef CDs. Inset: shows photographs of the solution of the CDs taken under visible light (left) and 365 nm UV light (right).

called electron traps. These new energy levels create different pathways for the excited electron to return to the ground state. In other words, when exciting CDs with a specific wavelength, a certain energy level is involved in the fluorescence emission. However, by changing the excitation wavelengths, different energy levels act as electron traps [44]. Thus, it can generally be suggested that both size factors and, functional groups are involved in this intrinsic behavior of CDs.

### Investigating the Selectivity of Four Batches of CDs and the Reason for Choosing Beef CDs

The selectivity of these four batches of CDs to drugs, amino acids and, ions was investigated by adding 100  $\mu\text{l}$  of 0.10 mM drugs, amino acids and ions to the CDs and

phosphate buffer solution. The results show that none of the drugs, amino acids and, ions significantly reduced (Figs. S5-7) the fluorescence of all four CDs, except for KTF (Fig. 3), which only significantly reduced the emission of fluorescence in CDs made from the beef. The surface functional groups of the CDs made from beef, beef liver, shrimp and oyster, were investigated using FT-IR spectroscopy. The intense peak corresponding to N–H stretching vibration of amine groups can be seen at  $1592\text{ cm}^{-1}$ , just observed in the FT-IR spectrum of beef CDs, which can act as an N-doping precursor. Nitrogen\_doping significantly enhanced the PL of the beef CDs toward beef liver, shrimp and, oyster CDs. Heteroatom doping not only improves the PL of the CDs, but also causing the functionalization surface of CDs to interact selectively with particular analytes, facilities (Fig. S2) [45-48].

This indicates a very high selectivity of CDs prepared from beef toward KTF. Among the prepared CDs, therefore, the beef was used to measure KTF in human plasma and urine samples after optimizing various parameters.

### Fluorescence Response of CDs to Ketotifen Fumarate

The fluorescence quenching response was described using the Stern-Volmer equation with the formula:

$$F_0 / F = I + k_{SV}C \quad (2)$$

Where  $F_0$  and  $F$  are fluorescence intensities in the absence and presence of KTF, respectively.  $k_{SV}$  is the Stern-Volmer PL quenching constant that indicates the sensitivity of the sensing platform to the quencher ( $C$ ).  $C$  is the concentration of KTF [49]. The Stern-Volmer plot is shown in Fig. 4. The proposed mechanism of this phenomenon can be justified based on the interaction of the functional groups of the CDs and KTF. In the absence of KTF, the fluorescence of CDs is affected by energy trapping by functional groups on the surface of CDs. KTF can interact with surface groups of CDs, such as  $\text{COO}^-$ , to quench the fluorescence. Figure (S8) shows the FT-IR spectra, of CDs and, KTF alone and in the presence of each other. Changes in the spectra in the range of  $1592$ ,  $1305$ , and  $3393\text{ cm}^{-1}$ , which are suggested to

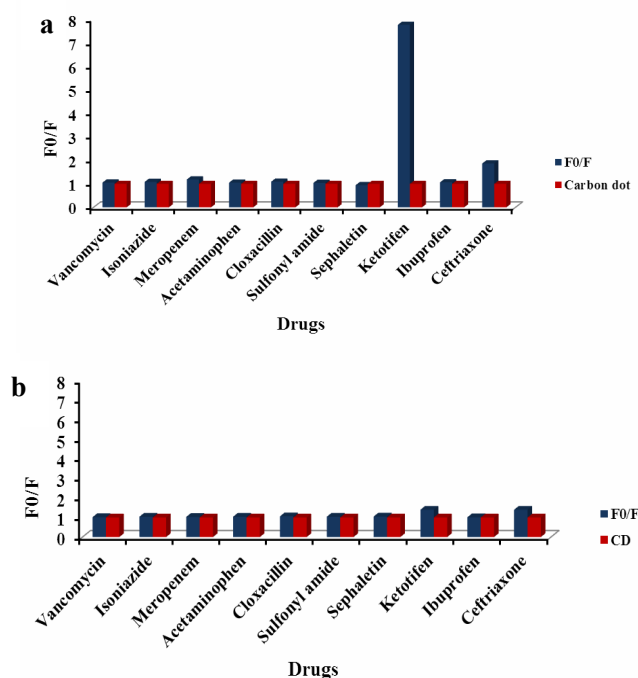


**Fig. 3.** Selectivity of (a) beef, (b) beef liver, CDs toward drugs with the concentration of 0.10 mM.

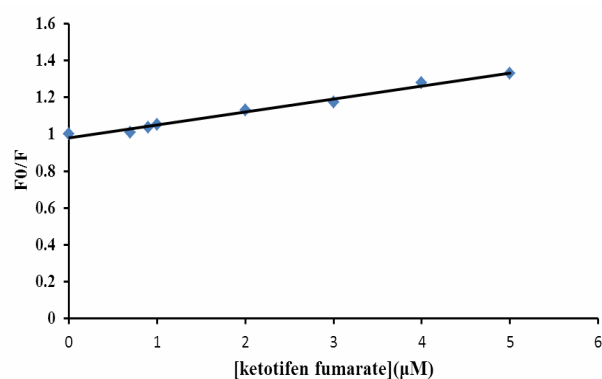


**Fig. 4.** Stern-volmer plot for fluorescence quenching of beef CDs by ketotifen fumarate

be related to the  $\text{COO}^-$ , C-OH and OH group tensile vibration, respectively, could indicate the interaction of KTF with CDs. The S group in KTF has a strong tendency to interact with  $\text{COO}^-$  due to the presence of free electron

pairs and interfering with the energy trapping of CDs performed by functional groups, which is a factor in the formation of fluorescence and interferes with the formation of new bonds or the filling of voids with electrons.

### Optimization of Experimental Conditions

In this section, the parameters including: pH, the concentration of buffer, amount of CDs and, incubation time are optimized to obtain the maximum sensitivity for the determination of KTF (Fig. 5).

The effect of pH on the fluorescence response of CDs was investigated by recording changes in fluorescence intensity of CDs in the pH range of 6-9 using phosphate buffer solution (Fig. 5a). A pH = 8 was selected as the optimal value for further measurements. Changing the pH can affect the strength, electronization, and electron attraction properties of the functional groups on the surface of CDs. CDs have carboxyl groups on their surface. The electron-withdrawing properties of carboxylic groups in an acidic solution can increase the energy separation between the agent energy levels, in which the excited electron is located, and the energy level at which the electron deficiency (cavity) is present. This increase in the separation can interfere with the electron-cavity fusion mechanism and ultimately reduce the emission of fluorescence carboxyl groups, which can also be protonated in an acidic solution [50]. In this case, the CDs stick together, which reduces the emission of fluorescence. In a base solution,  $\text{COO}^-$  functional groups on the surface of CDs can prevent electron-stimulated electron coupling at the level of conduction with electron deficiency cavities in the capacity layer by filling the electron deficiency cavities. This behavior could also be the reason for the reduction in the release of the fluorescence of the CDs into the base solution [51,52]. The presented explanations can justify the further quenching of fluorescence at pH = 8, which is close to neutral pH.

To investigate an optimal volume of CDs, fluorescence spectra of 0.5-3 ml volumes of CDs with a concentration of 50 ppm with phosphate buffer were recorded before and after increasing KTF, followed by recording the graphs. Then, 1 ml of CDs was selected as the optimal value for further testing (Fig. 5b).

Different concentrations of phosphate buffer with

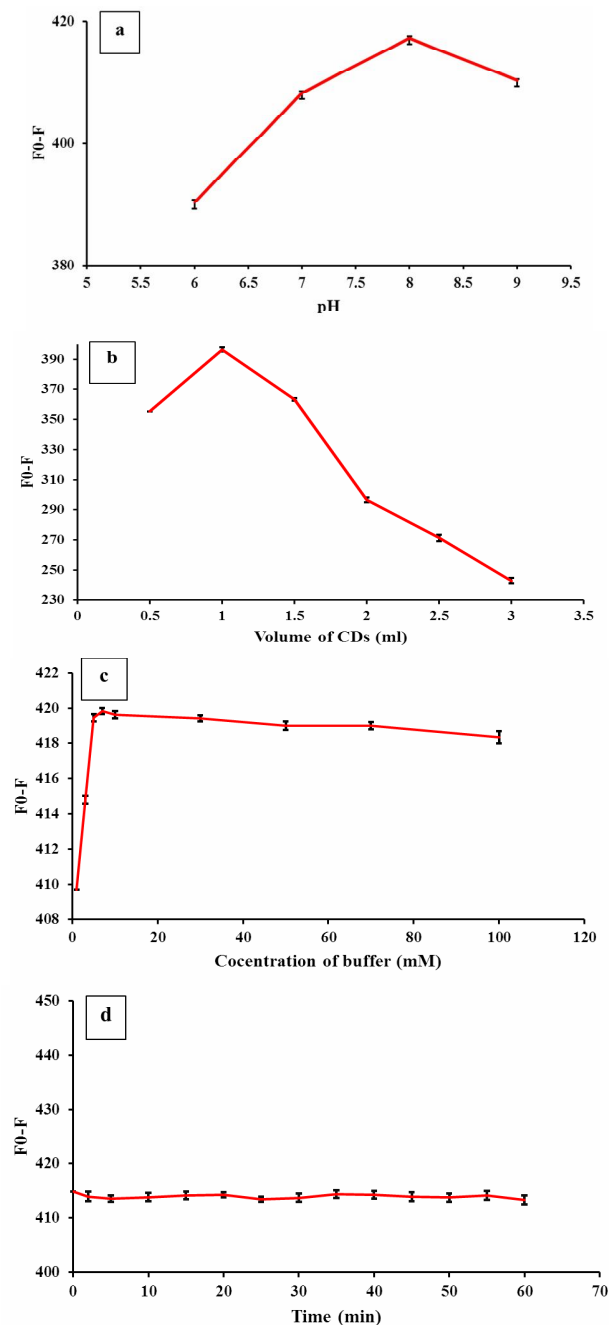


**Fig. 5.** Investigation of (a) pH, (b) CDs volume, (c) buffer concentration and (d) interaction time on fluorescence response. The concentration of beef CDs and ketotifen fumarate are (50 ppm and 100  $\mu\text{l}$ ), respectively, and volume of buffer phosphate is 1 ml. Error bars represent the standard deviation for three independent measurements.

(pH = 8) were prepared to investigate the effect of an optimal phosphate buffer concentration on the fluorescence response of CDs (Fig. 5c). The fluorescence emission spectrum of CDs was recorded in the presence of phosphate buffer with different concentrations in the range of 0.001-0.1 M in the presence and absence of KTF, and a concentration of 7 mM of phosphate buffer was selected as the optimal value.

Fluorescence emission spectra of optimal values were recorded at intervals of 1-60 min in the presence and, absence of KTF (Fig. 5d). It was observed that time did not significantly affect the interaction and all measurements were performed immediately.

### Analytical Figures of Merit

The optimal amounts of CDs and, phosphate buffer solution, *i.e.*, 1 (ml) of CDs solution and 1 ml of  $7 \times 10^{-3}$  M phosphate buffer solution (pH = 8), were added in the presence of various concentrations of KTF and the quenched fluorescence intensity was symmetrically increased with the concentration of KTF. The linear range was  $7.00 \times 10^{-7}$ - $5.00 \times 10^{-6}$  M with an estimated detection limit of  $3.00 \times 10^{-7}$  M (Fig. 6). As shown in Table 1, the suggested method has a suitable linear range, and the low detection limit values indicate that the proposed method is sensitive. The high correlation coefficient value of the regression equation which, is close to the unit, confirms the linearity of the calibration curve. The high values of the slope obtained from the calibration curve indicate the good sensitivity of the proposed method and the dependence of the effective factors on each other. Table 2 compares the experimental results of the proposed sensor with those previously reported for ketotifen fumarate determination in the literature. The detection sensitivity of this method is better than or comparable with others.

### Possible Fluorescence Quenching Mechanism

A series of investigations are carried out to explain the fluorescence quenching principle. As shown in Fig. S9a, the absorption peak of ketotifen fumarate completely overlaps with the excitation wavelength of CDs. It suggested that the fluorescence quenching of CDs may result from the inner filter effect (IFE). IFE occurs when the absorption spectrum

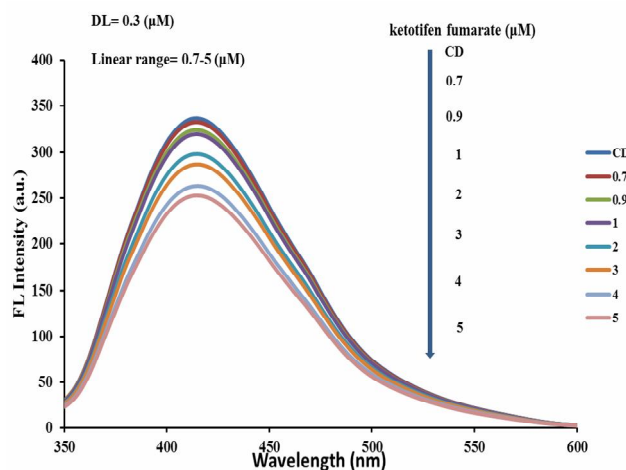


**Fig. 6.** Fluorescence spectra of the beef CDs (1 ml, 50 ppm) immediately, after addition of various concentration of ketotifen fumarate (from top to bottom: *i.e.*, 0, 0.7, 0.9, 1, 2, 3, 4 and 5  $\mu$ M).

**Table 1.** Investigation of Statistical Parameters of Calibration Curve of Ketotifen Fumarate Measurements

Parameters	Statistical results
Linear range (M)	$7.00 \times 10^{-7}$ - $5.00 \times 10^{-6}$
Maximum wavelength (nm)	330
Detection limit (M)	$3.00 \times 10^{-7}$
Slope (m)	18.29
Correlation coefficient (r)	0.98

of the quencher in the detection system overlaps with the excitation or emission spectra of CDs. To further confirm the primary reason for the FL quenching of CDs, corrections are made with the following equation (Eq.):

$$\frac{F_{cor}}{F_{obs}} = 10^{\frac{A_{ex} + A_{em}}{2}} \quad (3)$$

Where  $F_{obs}$  is the observed fluorescence intensity,  $F_{cor}$  is the corrected fluorescence intensity after removing IFE from  $F_{obs}$ .  $A_{em}$  and,  $A_{ex}$  are the absorbances at the maximum

**Table 2.** Limit of Detection (LOD) and Linear Range Comparison of some Ketotifen Fumarate Determination Method

System	Detection method	Linear range (M)	LOD ( $\mu\text{M}$ )	Ref.
Low pressure mercury lamp	Flow injection	$0.01 \times 10^{-3}$ - $10.00 \times 10^{-3}$	0.99	[54]
Cerium(IV) sulfate	AYAH 6SX1-T-1D CFI analyzer	$5.00 \times 10^{-3}$ - $10.00 \times 10^{-3}$	2.60	[55]
Bromophenol blue reagent	Spectrophotometric	$9.00 \times 10^{-6}$ - $37.60 \times 10^{-6}$	0.37	[56]
Modified carbon paste electrode	Potentiometric titration method	$1.00 \times 10^{-5}$ - $1.00 \times 10^{-2}$	1.42	[57]
Flow injection analysis	ISNAG-Fluorimeter	$1.00 \times 10^{-6}$ - $45.00 \times 10^{-6}$	29.70	[58]
CDs-based nanoprobe	Fluorescence	$7.00 \times 10^{-7}$ - $5.00 \times 10^{-6}$	0.30	This work

**Table 3.** Results of Recovery Studies of Ketotifen Fumarate from Human Plasma and Urine Samples

Urine samples							
Sample	Intra-day variation				Inter-day variation		
	Added ( $\mu\text{M}$ )	Found ( $\mu\text{M}$ )	Recovery (%)	RSD (n = 3) (%)	Found ( $\mu\text{M}$ )	Recovery (%)	RSD (n = 3) (%)
Urine a	0.00	N.D. <sup>a</sup>	-	-	N.D.	-	-
	0.50	0.48	96.00	3.20	0.47	95.80	3.80
	2.00	1.89	94.50	3.80	1.88	-	4.30
Urine b	0.00	N.D.	-	-	N.D.	-	-
	1.00	0.98	98.00	2.80	0.97	97.80	3.50
	4.00	3.95	98.75	3.60	3.92	98.20	3.20
Human plasma samples							
Sample	Added ( $\mu\text{M}$ )	Found ( $\mu\text{M}$ )	Recovery (%)	RSD (n = 3) (%)	Found ( $\mu\text{M}$ )	Recovery (%)	RSD (n = 3) (%)
Human plasma a	0.00	N.D.	-	-	N.D.	-	-
	1.50	1.42	94.60	4.25	1.43	95.50	3.30
	3.00	2.80	93.30	3.70	2.78	92.80	4.80
Human plasma b	0.00	N.D.	-	-	N.D.	-	-
	1.00	0.97	97.00	2.80	0.96	96.80	3.10
	3.00	2.98	99.33	3.80	2.97	99.21	5.30

<sup>a</sup>Not detected.

excitation wavelength ( $\lambda_{\text{em}} = 416 \text{ nm}$ ) and, maximum emission wavelength ( $\lambda_{\text{ex}} = 330 \text{ nm}$ ), respectively. Figure (S9b) shows the observed and corrected fluorescence quenching efficiencies ( $E_{\text{obs}}$  and  $E_{\text{cor}}$ ) versus different concentrations of ketotifen fumarate. The results illustrate that approximately 95% of the quenching effect comes from IFE [53].

### Analysis of Real Sample

To estimate the efficiency and percentage of the produced sensor recovery, in real samples, serum samples

of human albumin were obtained from Imam Khomeini hospital (Urmia) and urine samples were used after preparation. To test the recovery rate on real samples, certain values with specific concentrations of KTF were spiked and the fluorescence intensity was measured afterward. The obtained results reveal that the obtained concentrations are consistent with the added values. They indicate the non-interference of the real samples matrix compared to the analysis results of deionized water samples. (Table 3) The results of the above test (Table 3) show that the sensor made to measure the KTF is very accurate and

repeatable.

The proposed method was applied to the determine of ketotifen fumarate in a pharmaceutical formation (KETRAM 1 mg tablet). The obtained amount by the proposed method was 0.99 which, is in excellent agreement with the labeled value.

## CONCLUSIONS

In this test, a green, simple, cost-effective and highly selective spectrofluorimetric method is proposed for measuring KTF in human plasma and urine samples without the need for any extraction or preparation based on the quenching fluorescence of CDs by KTF. The fluorescence of CDs was significantly reduced by increasing KTF. The proposed method has satisfactory accuracy, high sensitivity, short response time, broad linear range, and, low detection limit. CDs made from natural materials (beef) are not toxic and are much more environmentally friendly.

## REFERENCES

- [1] S. Baker, G. Baker, *Angew. Chem.* 49 (2010) 6726.
- [2] H. Li, Z. Kang, Y. Liu, S. Lee, *Mater. Chem.* 22 (2012) 24230.
- [3] P. Zuo, X. Lu, Z. Sun, Y. Guo, H. He, *Microchim. Acta* 183 (2016) 519.
- [4] M. Shamsipur, A. Barati, S. Karami, *Carbon.* 124 (2017) 429.
- [5] Q. Wu, Q. Long, H. Li, Y. Zhang, S. Yao, *Talanta* 136 (2015) 47.
- [6] Y. Li, J. Xu, C. Sun, *RSC Adv.* 5 (2015) 1125.
- [7] J.D. Liu, J.J. Liu, J.H. Yuan, G.H. Tao, D.S. Wu, X.F. Yang, L.Q. Yang, H.Y. Huang, L. Zhou, X.Y. Xu, J.J. Hu, Z.X. Zhuang, *Toxicol Lett.* 212 (2012) 307.
- [8] S. Soltani, P. Zakeri-Milani, M. Barzegar-Jalali, M. Jelvehgari, Iran. *J. Basic Med. Sci.* 19 (2016) 550.
- [9] M. Zhou, Y.J. Li, Y.J. Ma, W.F. Wang, J. Mi, H. Chen, *Lumin.* 26 (2011) 319.
- [10] M. Joshi, A. Misra, *Int. J. Pharm.* 223 (2001) 15.
- [11] A. Akhavan, H. Karimi-Sari, M. Khosravi, E. Arefzadeh, M. Yavarahmadi, *Int. Forum. Allergy Rhinol.* 5 (2015) 386.
- [12] K. Smets, J. Werbrouck, A. Goossens, L. Gilissen, *Contact Derm.* 76 (2017) 124.
- [13] M. Abounassif, H. El-Obeid, E. Gadkariem, *J. Pharm. Biomed.* 36 (2005) 1011.
- [14] I. Miki, A. Kusano, S. Ohta, *Cell Immunol.* 171 (1996) 285.
- [15] J. Greiner, T. Mundorf, H. Dubiner, *Am. J. Ophthalmol.* 136 (2003) 1097.
- [16] G.J. Bustos, D. Bustos, O. Romero, *Clin. Exp. Allergy.* 25 (2005) 568.
- [17] G. Chen, H. Qu, Yaowu Fenxi Zazhi. 33 (2003) 123.
- [18] D. Yang, X. Qiang, C. Ji, B. Ru, *Acta. Pharmol. Sin.* 24 (2003) 1039.
- [19] C. Gui, Q. Hua, *J. Pharm. Anal.* 23 (2003) 123.
- [20] N. Kyung, J. Sung, P. Ji, *J. Pharm. Invest.* 42 (2012) 22010.
- [21] S. Muralidharan, L. Han, Y. Ming, J. Lau, K. Salishni, S. Arumugam, *Int. J. Pharm. Chem. Biol. Sci.* 2 (2012) 392.
- [22] M. Semreen, *Bull. Pharm. Sci.* 28 (2005) 291.
- [23] M. Elsayed, *Drug Dev. Ind. Pharm.* 32 (2006) 457.
- [24] M. Ansari, M. Kazemipur, A. Mohammed, *J. Pharm. Pharmacol.* 58 (2006) 106.
- [25] C.S.P. Sastry, P. Naidu, *Indian drugs.* 35 (1998) 147.
- [26] D. Atole, H. Rajput, *Innovare J. Sci.* 11 (2017) 59.
- [27] M. Amanlou, M. Hoseinzadehnazlou, H. Azizian, E. Souri, H. Farsam, *Anal. Lett.* 40 (2007) 3267.
- [28] W. Ciesilski, R. Zakrzewski, U. Zlobinsk, *Pharmazie.* 60 (2005) 237.
- [29] A. Mokhtari, M. Ghazaeian, M. Maghsoudi, M. Keyvanfard, I. Emami, *Luminescence* 30 (2015) 1094.
- [30] E. Farg, G. Mohamed, M. Khalil, M. Hwehy, *Anal. Chem.* (2011) 530.
- [31] M. Shamsipur, K. Molaei, F. Molaabasi, S. Hosseinkhani, N. Alizadeh, M. Alipour, S. Moassess, *Sens Actuators B Chem.* 257 (2018) 772.
- [32] J. Jiang, G. Oberdorster, P. Biswas, *J. Nanopart. Res.* 11 (2008) 77.
- [33] H. Sis, M. Brinci, *Colloids Surf. A Physicochem. Eng. Asp.* 341 (2009) 60.
- [34] H. Li, Y. Zhang, L. Wang, J. Tian, X. Sun, *Chem. Commun.* 47 (2011) 961.
- [35] M.J. Bojdys, O. Müller, M. Antonietti, A. Thomas,

- Chem. Eur. J. 14 (2008) 8177.
- [36] W. Lu, X. Qin, S. Liu, G. Chang, Y. Zhang, Y. Luo, *Economical, Anal. Chem.* 84 (2012) 5351.
- [37] Y. Gong, B. Yu, W. Yang, X. Zhang, *Biosens. Bioelectron.* 79 (2016) 822.
- [38] A. Samantara, S. Maji, A. Ghosh, B. Bag, R. Dash, B. Jena, *Mater. Chem.* 4 (2016) 2412.
- [39] V. Ramanan, S.K. Thiyagrajan, K. Raji, R. Suresh, R. Sekar, P. Ramamurthy, *Am. Chem. Soc.* 9 (2016) 4724.
- [40] Y. Qui, D. Gao, H. Yin, K. Zhang, J. Zheng, L. Wang, L. Xia, Q. Fu, *Sens Actuators B Chem.* 324 (2020).
- [41] J. Bhamore, S. Sha, T. Park, S. Kailasa, *Photochem. Photobiol.* 191 (2019) 150.
- [42] Y. Liu, M. Park, S. Park, Y. Zhang, M. Akanda, B. Park, H. Kim, *Carbon Lett.* 21 (2017) 61.
- [43] H. Xu, X. Yang, G. Li, C. Zhao, X. Liao, *Agric. Food Chem.* 63 (2015) 6707.
- [44] Y. Zhang, Y. Li, X.P. Yan, *Anal. Chem.* 81 (2009) 5001.
- [45] Y. Liu, Q. Zhou, Y. Yuan, Y. Wu, *Carbon* 115 (2017) 550.
- [46] C. Liu, P. Zhang, F. Tian, W. Li, W. Liu, *J. Mater. Chem. A* 21 (2011) 13163.
- [47] S. Gao, Y. Chen, H. Fou, X. Wei, C. Huo, L. Qu, *J. Mater. Chem. A* 2 (2014) 6320.
- [48] Y. Dong, H. Pang, H. Yang, C. Guo, J. Shao, Y. Chi, C. Li, T. Yu, *Angew. Chem. Int. Ed.* 52 (2013) 7800.
- [49] H. Xu, X. Yang, G. Li, C. Zhao, X. Liao, *J. Agric. Food Chem.* 63 (2015) 6707.
- [50] A. Scirtino, E. Martino, B. Dam, P. Schell, M. Cannas, F. Messina, *J. Phys. Chem.* 7 (2016) 3419.
- [51] M.J. Bojdys, J.O. Müller, M. Antonietti, A. Thomas, *Chem. Euro. J.* 14 (2008) 8177.
- [52] W. Lu, X. Qin, S. Liu, G. Chang, Y. Zhang, Y. Luo, *Economical, Anal. Chem.* 84 (2012) 5351.
- [53] S. Chen, Y. Yu, J. Wang, *Anal. Chim. Acta* 999 (2018) 13.
- [54] M. Al-banna, *Sys. Rev. Pharm.* 11 (2020) 305.
- [55] N. Awadie, M. Ibraheem, *Int. J. Res. Pharm. Chem.* 6 (2016) 411.
- [56] O. Al-Khazrajy, *Pure Appl. Sci. Technol.* 24 (2011) 25213407.
- [57] M. Khater, Y. Issa, S. Mohamed, *Drug Test Anal.* 5 (2013) 74.
- [58] S. Nagam, Q. Hayder, *Baghdad Sci. J.* 16 (2019) 353.